Journal of Materials Chemistry B

PAPER

Cite this: J. Mater. Chem. B, 2014, 2, 7945

The aligned core–sheath nanofibers with electrical conductivity for neural tissue engineering†

Jianguang Zhang,[a] Kexin Qiu,[ab] Binbin Sun,[a] Jun Fang,[ab] Kuihua Zhang,[c] Hany El-Hamshary,[d] Salem S. Al-Deyab[d] and Xiumei Mo*[ab]

Received 18th July 2014
Accepted 11th September 2014

DOI: 10.1039/c4tb01185f

www.rsc.org/MaterialsB

Currently, electroactive biomaterials have often been fabricated as tissue engineering scaffolds to provide electrical stimulation for neural tissue engineering. The goal of this work was to study the synergistic effect of electrical stimulation and nerve growth factor (NGF) on neuron growth. The composite meshes of polyaniline (PANi) and well-blended poly(L-lactic acid-*co*-ε-caprolactone)/silk fibroin (PS) incorporated with nerve growth factor (NGF) were prepared by coaxial electrospinning. The results showed that the increased concentration of PANi had a large effect on the fiber diameter, which was significantly reduced from 683 ± 138 nm to 411 ± 98 nm and then increased to 498 ± 100 nm. The contact angles and Young's modulus decreased to 28.3° ± 5.4° and 7.2 ± 1.2 MPa, respectively, and the conductance increased to 30.5 ± 3.1 mS cm^{-1}. The results of the viability and morphology of mouse Schwann cells on the nanofibrous meshes showed that PS-PANi-1 loaded with NGF exhibited the highest cell number after 5 days culture and the aligned nanofibers could guide cell orientation. The synergistic effects of electrical stimulation and NGF were also investigated *via* the growth and differentiation of rat pheochromocytoma 12 (PC12) cells. The scaffolds loaded with NGF under electrical stimulation could effectively support PC12 neurite outgrowth and increase the percentage of neurite-bearing cells as well as the median neurite length. More importantly, the NGF release from the conductive core–shell structure nanofiber could be increased by electrical stimulation. These promising results demonstrated that there was a potential use of this functional scaffold for nerve tissue regeneration.

1 Introduction

Peripheral nerve injury is a common clinical disease and most clinical injuries are associated with nerve gaps, which cannot be repaired by end-to-end sutures directly.[1] However, because of the limited supply of autografts, which are the clinical "gold standard" for bridging nerve gaps, it is impossible to satisfy the increasing demand for clinical nerve repair. To overcome the limitations associated with peripheral nerve autografts, biomaterials play a pivotal role in nerve regeneration processes. Many studies have focused on developing more effective biomaterials to promote nerve regeneration. Recent research showed that some biological tissues exhibit electrical activities for modulating cellular fate, processes and behaviors, and electrical stimulation through conductive scaffolds can promote cell proliferation and differentiation, specifically for neural, cardiac and muscle tissues.[2–4] Therefore, electrically conductive materials as scaffolds for nerve regeneration have gained more attention.[5] Typically, conductive polymers were often used as fillers in composite systems, such as polypyrrole (PPy), polythiophene (PT), polyaniline (PANi), poly(3,4-ethylenedioxythiophene) (PEDOT) and multiwalled carbon nanotubes (MWCNTs), and most of these have been studied for biological applications.[6–11]

PANi has been chosen as the scaffold material for its low cost and controllable conductivity. It has been recognized as a promising scaffold material and widely investigated in neural, cardiac and skeletal muscle tissue engineering. However, pure PANi is brittle, rigid and difficult to form into a nerve guidance substrate. Electrospinning is a promising approach to fabricate nanofibers, which can mimic the native extracellular matrix (ECM). The choice of electrospun fibers as a drug-delivery vehicle had an added incentive in that they possess large surface areas and interconnected pores for tissue ingrowth.[12,13] In addition, many researchers have reported that aligned electrospun scaffolds were able to provide contact guidance to cultured cells, resulting in an elongation and alignment of cells along the

[a]College of Chemistry, Chemical Engineering and Biotechnology, Donghua University, Shanghai, 201620, People's Republic of China

[b]State Key Laboratory for Modification of Chemical Fibers and Polymer Materials, College of Materials Science and Engineering, Donghua University, Shanghai, 201620, People's Republic of China

[c]Department of Polymer Materials, College of Materials and Textile Engineering, Jiaxing University, Zhejiang, 314001, People's Republic of China

[d]Department of Chemistry, College of Science, King Saud University, Riyadh 11451, Kingdom of Saudi Arabia

† Electronic supplementary information (ESI) available. See DOI: 10.1039/c4tb01185f

major axis of the nanofibers.[14–17] In order to integrate the electrical, mechanical and biological properties, nanofibrous conductive scaffolds based on blends of PANi with other degradable polymers were created by electrospinning. Li *et al.* reported that PANi-gelatin blend fibers supported H9c2 rat cardiac myoblast cell attachment and proliferation.[18] Shin *et al.* demonstrated that the PANi/poly(L-lactic acid-*co*-ε-caprolactone) (P(LLA-CL)) nanofibers could improve cell adhesion on the substrate and enhance NIH-3T3 fibroblast growth under electrical stimulation.[19] Moreover, the electrical conductivity of the fibers affected the differentiation of PC12 cells.[20] Sung *et al.* developed aligned PANi/poly(lactic-*co*-glycolic acid) (PLGA) nanofibers, which were used for coordinating the beating of cultured cardiomyocytes synchronously, and neonatal rat cardiomyocyte clusters could be coupled together through electrical stimulation.[21] The electrically conductive aligned poly(ε-caprolactone) (PCL)/PANi nanofibers further enhanced myotube maturation.[22]

Based on our previous research, silk fibroin (SF) was an excellent candidate for generating tissue engineering scaffolds. Due to its good biocompatibility, biodegradability and minimal inflammatory reactions, electrospun nanofibers of SF and its blends have been widely used for tissue engineering.[23] We fabricated aligned SF/P(LLA-CL) nanofibrous meshes, and then reeled them into nerve guidance conduits to promote peripheral nerve regeneration. The results demonstrated that blending SF into P(LLA-CL) greatly improved nerve regeneration.[24,25] In addition, neurotrophic factors, such as nerve growth factor (NGF), played a critical role in nerve regeneration. However, NGF was labile and had a short half-life *in vivo*. Additionally, only a small amount of growth factors (picograms to nanograms) was often required to elicit biological activity, and the excess NGF might cause possible side effects. In order to maintain a stable NGF concentration, sustained release of NGF was needed.[26,27] Wang *et al.*[13] incorporated NGF into aligned core–shell nanofibers by coaxial electrospinning, and sustained release was observed for one month. According to previous research,[8,28] electrical stimulation and neurotrophin could have dramatic effects on nerve regeneration. However, aligned core–shell nanofibers incorporated with NGF and electrical properties to promote neurite outgrowth have not been reported.

The aim of this work was to fabricate a new type of scaffold which comprised conductive polyaniline (PANi) and well-blended poly(L-lactic acid-*co*-ε-caprolactone) (P(LLA-CL))/silk fibroin (PS) incorporated with NGF by coaxial electrospinning, in which NGF was used as the core material and PS/PANi was used as the shell material to elucidate the synergistic effects between electrical stimulation and the nerve growth factor on neurite outgrowth of PC12 cells.

2 Experimental

2.1 Materials

The co-polymer of poly(L-lactic acid-*co*-ε-caprolactone) (P(LLA-CL)) (M_w = 300 kDa, LA : CL = 50 : 50) was purchased from Gunze Limited (Japan). Bombyx mori silkworm cocoons were supplied by Jiaxing Silk Co. Ltd. (China) and the regenerated silk fibroin (SF) was prepared as in previous reported methods.[29] 1,1,1,3,3,3-Hexafluoro-2-propanol (HFIP) and PANi emeraldine base (PANi-EB) of MW 15 kDa were purchased from Alfa Aesar Company, USA. Camphor sulfonic acid (CSA) was purchased from Sigma-Aldrich. Cell culture reagents including fetal bovine serum (FBS), horse serum (HS), Dulbecco's modified Eagle's medium (DMEM), phosphate-buffered saline (PBS), trypsin/EDTA, RPMI 1640 medium and penicillin–streptomycin were purchased from Gibco BRL, Life Technologies, USA. Fluorescein isothiocyanate-conjugated bovine serum albumin (FITC–BSA), nerve growth factor (NGF 2.5S, murine, natural) and the ELISA kit were purchased from Invitrogen (Carlsbad, CA, USA). Rat pheochromocytoma cells (PC12) and mouse Schwann cells were obtained from the Shanghai Institute of Biochemistry and Cell Biology (SIBCB, CAS, China).

2.2 Electrospinning

The PS solution (16 w/v%) was prepared by dissolving P(LLA-CL)/SF (w/w 75 : 25) in HFIP, and the conductive PANi solution (2.4 and 3.2 w/v%) was prepared by dissolving PANi-EB/CSA (w/w 50 : 50) in HFIP at room temperature (RT). CSA was used as a dopant to change the conductivity status of PANi from emeraldine base (insulator) to emeraldine salt (conductor).[30] Various PS/PANi electrospun solutions were blended from the same volume of the aforementioned PS solution and PANi solution. And the final compositions of the electrospun solutions are listed in Table 1.

Aligned PS/PANi nanofibers were prepared by electrospinning. Briefly, the prepared solutions were placed in a plastic syringe with a blunt-ended needle (21 G). The syringe was loaded in a syringe pump (789100C, Cole-Parmer Instruments, USA) operating at a rate of 1.0 mL h^{-1}. A voltage of 12 kV was generated by a high-voltage power supply (BGG6-358, BMEI Co. Ltd., China). To obtain aligned nanofibers, a rotating drum collector was used at a speed of 4000 rpm. The distance between the needle and the collector was 5–6 cm. The obtained PS/PANi meshes were placed in a desiccator saturated with 75% ethanol vapor at RT overnight, making the meshes insoluble in water.

NGF-loaded PS/PANi core–shell fibers were fabricated by coaxial electrospinning (Fig. S1†).[13] Unspecified parameters were used for preparing the aligned core–shell nanofibers with a slight change. A special coaxial stainless steel needle was used

Table 1 Compositions of electrospun PS/PANi solutions, mixed from equivalent volume of original PS solution (16 w/v%) with PANi solutions (0, 2.4, 3.2 w/v%)

	PS/PANi electrospun solution		
Sample	PS concentration (w/v%)	PANi concentration (w/v%)	PANi mass content (wt%)
PS-PANi-0	8	0	0
PS-PANi-1	8	1.2	13
PS-PANi-2	8	1.6	17

consisting of an inner 21 G needle and an outer 30 G needle, and the inner tip protruded 0.5 mm from the outer one, in which the core solution (100 μL β-NGF (100 μg mL^{-1}) added to 1 mL BSA (10 wt%)) and the shell solution (PS/PANi solution) were injected at the rate of 0.2 mL h^{-1} and 1 mL h^{-1}, respectively. Similarly, to observe the distribution of core components in the nanofibers, 200 μL FITC–BSA (5 wt%) was added to 900 μL BSA (10 wt%) and used as the core solution.[26]

2.3 Characterization of aligned nanofibrous meshes

Fiber morphology was observed with a scanning electron microscope (SEM, Hitachi TM-100, Japan). The average and standard deviation of the fiber diameter were calculated from 100 random measurements per image, and the angle distribution of the fibers and their major axis fluctuated in a wide range from 0° to 90° for each image (ImageJ software).[15,31] Laser scanning confocal microscopy (LSCM, Carl Zeiss LSM 700, Germany) was used for observing the distribution of FITC–BSA in the core of the PS/PANi nanofibers. Transmission electron microscopy (TEM, Hitachi H-800, Japan) at 100 keV was used for verifying the core–shell structure and the samples for TEM observation were prepared by collecting the nanofibers on carbon-coated Cu grids.[12] Fourier transform infrared spectra (FTIR) were obtained on an Avatar 380 FTIR instrument (Nicolet 6700, Thermo Fisher, USA). All spectra were recorded in transmission mode (32 scans) in the wavelength range of 4000 to 500 cm^{-1}.

The surface hydrophilicity of the electrospun nanofibers was studied by measuring the water contact angle (WCA) using a sessile drop method with distilled water (OCA40, Dataphysics, Germany).

Mechanical properties of fibrous samples (10×30 mm^2, $n = 5$) were measured on a universal materials tester (H5 K-S, Hounsfield, UK) at 20 °C with a humidity of 65%. The cross-head speed was set at 10 mm min^{-1}.

The conductivity of electrospun PS/PANi fibers (10×30 mm^2, $n = 5$) was measured using the cyclic voltammetry method in a three-electrode system (CHI660D, Chenhua Ltd., China) at RT. The constant current applied to the surface created a differential voltage and then the conductivity of each mesh was calculated by the equation $\sigma = L/RS$ (σ, electrical conductivity, S cm^{-1}; L, distance between counter and working electrodes, cm; R, ohmic resistance, Ω; and S, cross-sectional area of sample, cm^2). To investigate the electrically conductive stability of the electrospun samples, each sample (10×30 mm^2, $n = 5$) was immersed in 2 mL serum-free RPMI 1640 medium in a centrifuge tube and the tubes put onto a shaking table at 37 °C (60 rpm) for up to 1, 3, 7, and 14 days. And the collected samples were rinsed several times with deionized water to remove residual medium and dried under a vacuum for measurement of electrical resistivity.[8,20,30]

2.4 Cell proliferation and morphology

The mouse Schwann cells were used to study cell proliferation and differentiation on nanofibers. The cells were cultured in DMEM supplemented with 10% FBS and 1% penicillin–streptomycin at 37 °C with 5% CO_2 in a humidified atmosphere. For cell culture, the circular samples (15 mm diameter, collected on the round glass coverslips) were sterilized with 75% ethanol and UV, then washed with PBS three times in 24-well plates. The cells were seeded onto the electrospun PS/PANi fibers and tissue culture plate (TCP) at a density of 1×10^4 cells per well. The medium was replaced every three days.

The 3-(4,5-dimethylthiazol-2-yl)-2,5-diphenyltetrazolium bromide (MTT, Sigma-Aldrich, USA) assay was used to measure the cell cytotoxicity after seeding for 1, 3, and 5 days. Briefly, MTT solution was added to each well, incubated for 4 h at 37 °C, and then replaced by dimethyl sulfoxide (DMSO, Sinopharm, China) to dissolve the formazan crystals. The absorbance of the solution was measured by the enzyme-labeled instrument (MK3, Thermo) at 492 nm.

For observing the cell morphology, after 5 days culture of mouse Schwann cells on nanofibers with a density of 8×10^3 cells per well, the scaffolds were washed with PBS to remove the residual medium and unviable cells, and fixed in 4% paraformaldehyde (Thermo Scientific) for 30 minutes. Fixed samples were rinsed with PBS three times (15 minutes each time) and blocked in 1% BSA (Sigma) for 30 minutes. Subsequently, the cells were labeled with Alexa Fluor 568 phalloidin (Life Technologies) for 20 minutes and further with 4′,6-diamidino-2-phenylindole (DAPI, Vectashield, Vector Laboratories, USA) for 5 minutes. The mounted samples were observed by LSCM.

2.5 PC12 cell culture and electrical stimulation

PC12 cells were cultured in RPMI 1640 medium supplemented with 15% HS, 2.5% FBS and 1% penicillin–streptomycin at 37 °C with 5% CO_2 in a humidified atmosphere. The samples were sterilized as in the above mentioned methods. The PC12 cells were seeded on the electrospun nanofibrous scaffolds at a density of 5×10^4 cells per well and allowed to adhere for 24 h. The device for electrical stimulation was similar to that previously described.[32] A constant voltage of 100 mV cm^{-1} was applied across the wires and along the fiber direction for 1 h per day (total 5 days). Nanofibers without growth factor or electrical stimulation were used as control.

2.6 Immunofluorescence image analysis

After 5 days incubation and electrical stimulation, the PC12 cells were fixed with 4% paraformaldehyde for 30 minutes and washed with PBS, then permeabilized in 0.1% Triton X-100 for 6 minutes and blocked in 1% BSA for 30 minutes. The fluorescence staining method followed the above mentioned method for Schwann cells. The mounted samples were observed by LSCM.

The median neurite length and the percentage of neurite-bearing PC12 cells were measured according to previous reported methods. More than 600 PC12 cells were analyzed by ImageJ software for each condition ($n = 4$).[6,8,33]

2.7 NGF release from PS/PANi composites

PS-PANi-1 + NGF fibers were used for an *in vitro* release study of NGF in the absence and presence of electrical stimulation

(a constant voltage of 100 mV cm^{-1}). Each electrospun sample (10×30 mm^2, ~24.8 mg) was soaked in a well of a 24-well plate filled with 400 μL serum-free RPMI 1640 medium at 37 °C. Half of the sustained-release medium was retrieved from the well and an equal volume of fresh medium was replaced at various time points. The amount of released NGF in the collected sustained-release medium was determined with an ELISA kit. Six samples were used for one condition at each time point.

PC12 cells were used to measure the bioactivity of the electrically stimulated NGF release from electrospun NGF-loaded PS/PANi fibers. PC12 cells were seeded at a density of 1×10^4 cells per well in a 24-well plate and cultured in a medium of 400 μL NGF sustained-release solution (5 days) with 600 μL RPMI 1640. Wells in 1 mL RPMI 1640 medium without NGF sustained-release solution were used as control. The 5 days sustained-release medium used here was with or without electrical stimulation. Optical images of the PC12 cells were taken after culture for 3 days.

2.8 Statistical analysis

All of the data were expressed as means ± standard deviation. Statistical analysis was carried out using one-way ANOVA (Origin 8.0) and a value of $p < 0.05$ was considered to be statistically significant.

3 Results and discussion

3.1 Morphology and characterization of electrospun nanofibers

The compositions of aligned nanofibrous meshes are summarized in Table 1. It was observed that the color of the meshes became emerald when PANi was added to the complex composites (Fig. S1†). Fig. 1 shows the morphology and alignment of electrospun PS/PANi nanofibers. As shown in Fig. S2,† the average diameter of electrospun fibers significantly decreased from 683 ± 138 nm to 411 ± 98 nm for PS-PANi-0 and PS-PANi-1 nanofibers and increased to 498 ± 100 nm for PS-PANi-2 nanofibers, respectively. Previous studies reported that the diameter of the nanofibers could be affected by the polymer concentration and solution conductivity as well as the dispersion of PANi under the same electrospinning parameters.[31,34] Similar results were also reported by Li *et al.* and Ghasemi-Mobarakeh *et al.*[18,30] However, in the present work, low-molecular-weight PANi with different concentrations was used to fabricate PS/PANi nanofibers. The addition of PANi to the PS solution increased the conductance and charge density of the solution, which caused the stronger elongation forces to lead to smaller diameters of the electrospun nanofibers. When the content of PANi reached 80 mg, the high solution viscosity resulted in an increase in nanofiber diameters.[10,35] In addition, the high viscosity also significantly affected the unstable nanofiber form during the electrospinning process, which might influence the mechanical properties of electrospun nanofibers.

The alignment of the electrospun fibers was characterized by statistical analysis of the angles between the fibers and their major axis. Fig. 1B reveals that the electrospun nanofibers exhibited better alignment with an increase in PANi concentration, and the angle of most nanofibers narrowed to 0 to 10°.

The hydrophilic characteristics of the scaffold could influence the cell adhesion and migration. Whereas the silk fibroin is hydrophilic, the incorporation of PANi slightly increased the hydrophilicity of the scaffolds. As shown in Table 2, the contact angles of each mesh were 80.2 ± 3.5°, 32.4 ± 7.9° and 28.3 ± 5.4° for PS-PANi-0, PS-PANi-1 and PS-PANi-2, respectively. The images of the water droplets could not be maintained for a longer time (shorter than 100 s).

TEM and LSCM were used to study the core–shell structure of the composite nanofibers. Fig. 2A shows TEM micrographs of

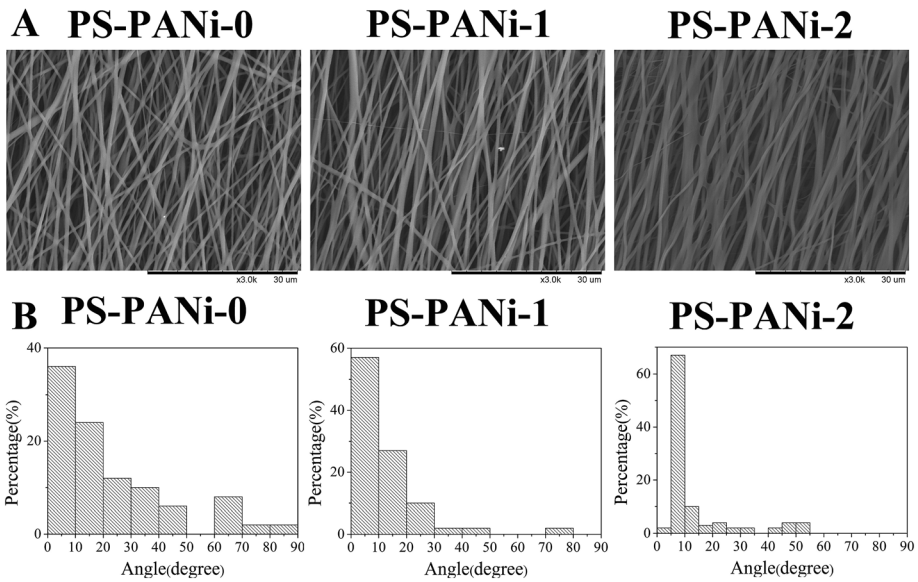

Fig. 1 (A) SEM images of PS/PANi nanofibers, (B) the histograms of the fiber angle distribution.

Table 2 Water contact angle values and image of water droplets on the surface of PS-PANi composites

Sample	Contact angle (°)	Image of drops
PS-PANi-0	80.2 ± 3.5	
PS-PANi-1	32.4 ± 7.9	
PS-PANi-2	28.3 ± 5.4	

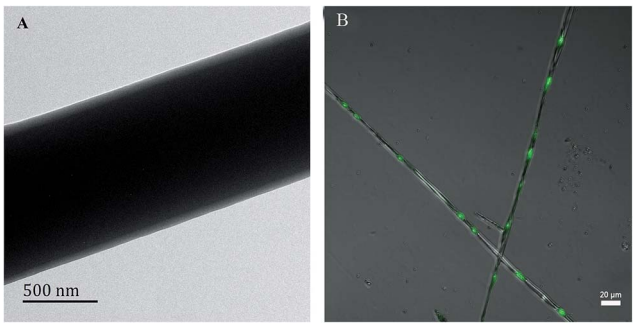

Fig. 2 (A) TEM micrographs of electrospun NGF-loaded PS/PANi core–shell nanofibers, (B) electrospun PS/PANi nanofibers with FITC–BSA. Scale bar = 20 μm.

the core–shell structure of PS/PANi in the shell and BSA + NGF in the core of the nanofibers, and Fig. 2B indicates the fiber emitted fluorescent light, suggesting the presence of FITC–BSA. The results confirmed that the NGF was successfully incorporated in the core of the nanofibers.

The mechanical properties of nanofibers are very important for effective application in tissue engineering. The average thicknesses of the PS-PANi-0, PS-PANi-1 and PS-PANi-2 meshes were 0.035, 0.032 and 0.037 mm, respectively. The mechanical properties of the PS/PANi composite nanofibers were characterized by tensile measurement. Fig. 3 represents the mechanical parameters of PS/PANi electrospun nanofibers, including the representative stress–strain, tensile strength, elongation at break and Young's modulus. As shown in Fig. 3A, all samples exhibited a linear elastic behavior. The tensile strength and elongation at break decreased with increasing content of PANi in the fibers. For example, the tensile strength decreased from 13.7 ± 1.5 MPa for PS-PANi-0 to 8.4 ± 1.2 and 5.7 ± 0.9 MPa for PS-PANi-1 and PS-PANi-2, respectively (Fig. 3B). The elongation at break of PS/PANi dropped from 120.3 ± 10.5% for PS-PANi-0 nanofibers to 116.9 ± 9.2% and 93.1 ± 5.3% for PS-PANi-1 and PS-PANi-2, respectively (Fig. 3C). These results were similar to previous studies.[29,33] However, compared with other studies,[22,31] we used low molecular weight PANi. In order to maintain the conductivity of nanofibers, more PANi was added to fabricate the PS/PANi fibers. Therefore, the Young's modulus of PS/PANi exhibited a similar trend, decreasing from 17.5 ± 1.9 MPa to 10.8 ± 1.7 MPa and finally to 7.2 ± 1.2 MPa for PS-PANi-0, PS-PANi-1 and PS-PANi-2, respectively (Fig. 3D). Although the elasticity decreased with increasing PANi, the composite nanofibers were still relatively elastic and suitable for nerve tissue engineering.

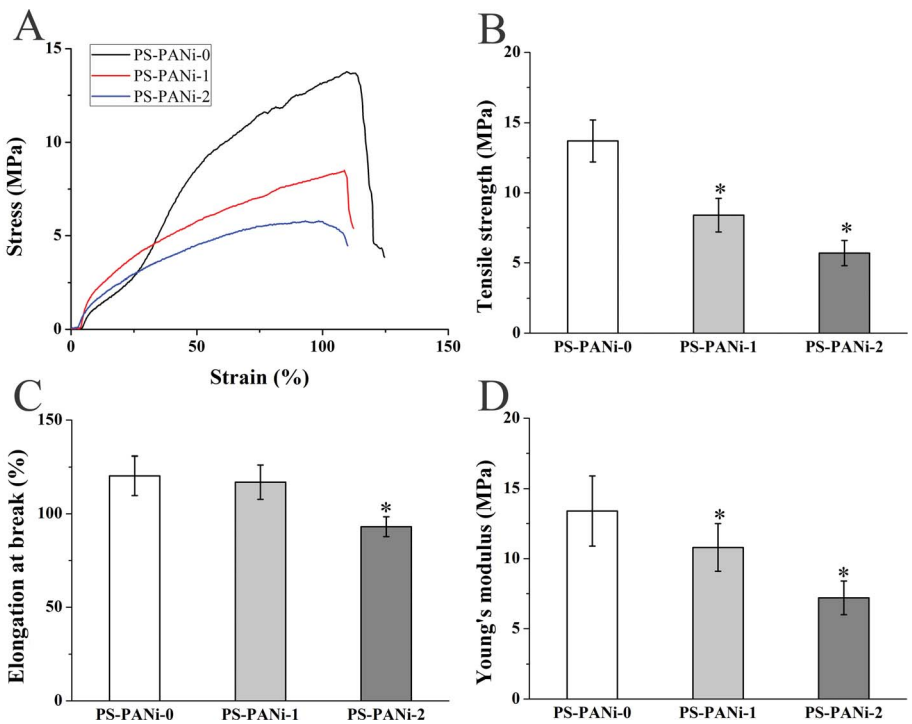

Fig. 3 Mechanical properties of electrospun PS/PANi nanofibers. (A) representative tensile stress–strain curves, (B) tensile strength at break, (C) elongation at break and (D) Young's modulus (* = significantly different in comparison with PS-PANi-0, $p < 0.05$, $n = 5$).

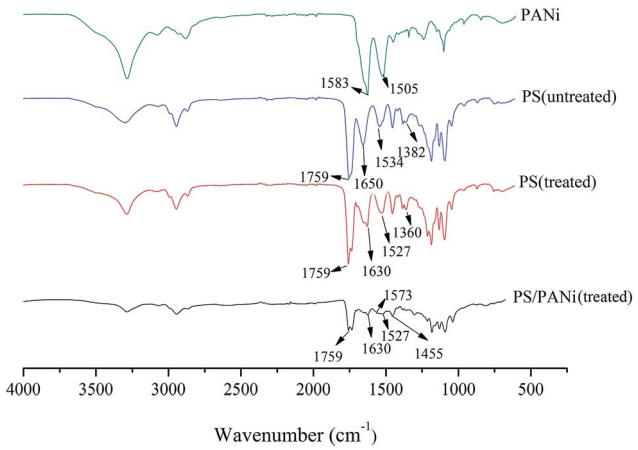

Fig. 4 ATR-FTIR spectra of electrospun PANi, PS, and PS/PANi fibers with and without ethanol vapor treatment.

The chemical characteristics of the electrospun nanofibers were determined by ATR-FTIR spectroscopy. Fig. 4 shows ATR-FTIR spectra of electrospun PANi, PS, and PS/PANi fibers with and without ethanol vapor treatment. The ATR-FTIR spectra present the two bands of C=C (stretching vibrations of diiminoquinoid and benzenoid) peaks of pure PANi at 1583 cm^{-1} and 1505 cm^{-1}, and the characteristic ester group stretching of P(LLA-CL) was at 1759 cm^{-1} (C=O),[19] implying the presence of PANi and P(LLA-CL). After adding the CSA, the PANi characteristic peaks were red-shifted to 1573 cm^{-1} and 1455 cm^{-1}, respectively, due to a significant increase in molecular dipole moment in the blended PS/PANi samples,[21,36] which suggested PANi was transformed from an insulator into a conductor and CSA was successfully doped into the composite fibers.[37] In addition, after the ethanol vapor treatment, the characteristic peaks of SF were shifted from 1650 to 1630 cm^{-1} for amide I, 1534 to 1527 cm^{-1} for amide II and 1382 to 1360 cm^{-1} for amide III, respectively, which represents the structural transition of SF from α-helix to β-sheet which made the meshes insoluble in water.[38,39]

Although the PANi reduced the mechanical properties of the nanofibers, the composite nanofibers possess good electrical properties. Fig. 5 shows the conductivity and electrical stability of the PS/PANi fibers. Compared with the undetectable conductivity of pure PS, the incorporation of PANi into the PS nanofibers significantly increased the conductivity, which increased from 18.2 ± 1.2 mS cm^{-1} (PS-PANi-1) to 30.5 ± 3.1 mS cm^{-1} (PS-PANi-2) as shown in Fig. 5A. The conductivity has not obviously changed during incubation in the media, but the profiles tend to decrease with increasing time, which might be due to the dopant leaching out from the scaffolds (Fig. 5B).[5,40] The results suggested that electrospun PS/PANi nanofibers could maintain their electrical property for at least 2 weeks.

3.2 Biocompatibility of the electrospun nanofibers

To research the effect of PANi incorporated with NGF on mouse Schwann cell proliferation, the MTT assay was performed. As shown in Fig. 6B, the number of cells cultured on NGF-loaded PS/PANi meshes was significantly higher than that on PS-PANi-0 ($p < 0.05$), and NGF-loaded PS-PANi-1 exhibited the highest cell number after 5 days culture. However, the proliferation of cells increased slowly on the PS/PANi scaffolds compared with TCP and the higher content of PANi resulted in reducing the number of cells cultured in PS-PANi-2. The study of PANi/P(LLA-CL) fibers showed similar initial adhesion and proliferation of C2C12 myoblasts among the nanofiber groups with different concentrations of PANi.[29] These results demonstrated that the high content of low-molecular-weight PANi induced cytotoxicity to Schwann cells, and the incorporation of NGF into PS/PANi nanofibers could enhance the proliferation and decrease the toxicity effect of PANi to Schwann cells.

We also investigated the morphology of Schwann cells on aligned nanofibers after 5 days of incubation. The representative confocal laser micrographs of Schwann cells on the scaffolds and TCP showed that Schwann cells spread well on the nanofibers (Fig. 6A). The density of cells cultured on PS-PANi-1 and PS-PANi-2 were higher than that on PS-PANi-0 and the number of cells cultured on NGF-loaded nanofibers was larger than that without NGF. Notably, the Schwann cells grew along the direction of conductive nanofibrous scaffolds compared with the case on TCP. Therefore, the aligned nanofibers could provide guidance to form an oriented cellular morphology, which plays an important role in nerve regeneration. The result

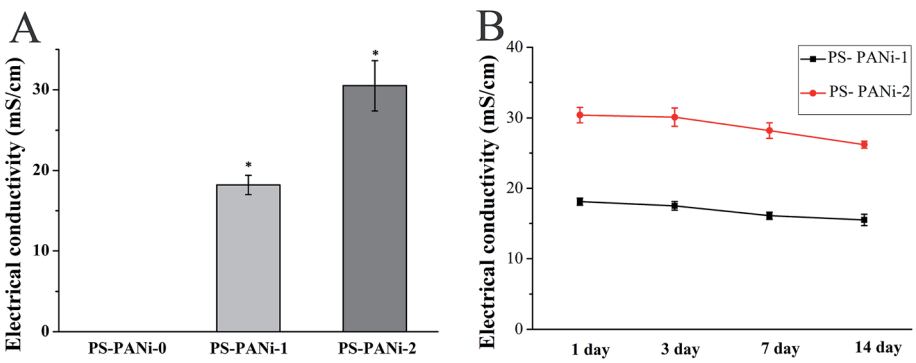

Fig. 5 Electrical conductivity of electrospun PS/PANi fibers (A) before and (B) after immersion in serum-free RPMI 1640 medium at 37 °C for up to 14 days (* = significantly different in comparison with PS-PANi-0, $p < 0.05$, $n = 5$).

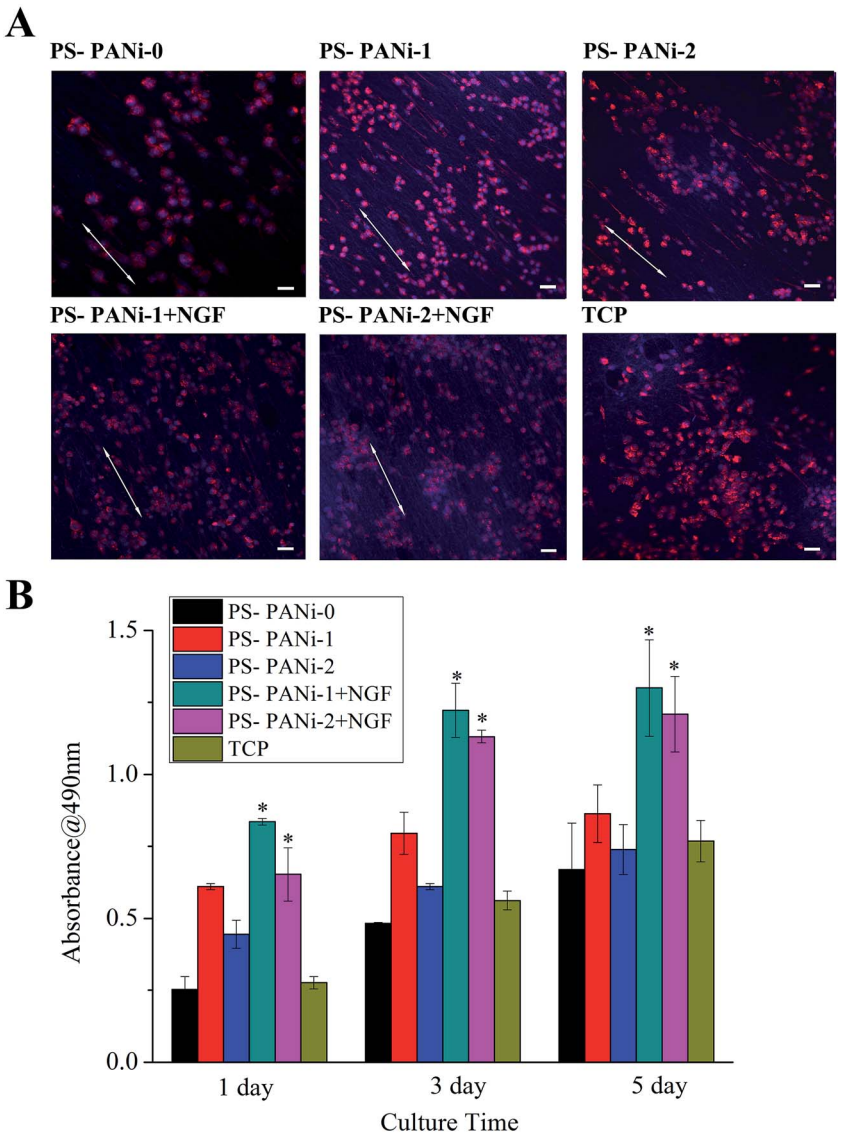

Fig. 6 (A) Representative confocal laser micrograph images of Schwann cells cultured on the aligned electrospun PS/PANi fibers with and without NGF loading at day 5 (scale bar = 10 μm) and TCPs were used as control. (B) MTT assay of Schwann cell proliferation (* = significantly different in comparison with PS-PANi-0, $p < 0.05$, $n = 3$).

illustrated that the aligned nanofibrous scaffolds provide a good microenvironment for nerve cell proliferation and could promote neurite extension.[41] Because pure PANi is brittle and marginally biodegradable and high contents of low-molecular-weight PANi would have a toxic effect on Schwann cells, therefore PS-PANi-1 and NGF-loaded PS-PANi-1 were selected for the following studies.

3.3 *In vitro* synergistic effect on PC12 cells

PC12 cells were used to evaluate the synergistic effect of electrical stimulation and nerve growth factor (NGF) on neuron growth.[9,42] The cells were allowed to adhere to the substrate for 24 h before being stimulated with 100 mV cm^{-1} for 1 h per day (total 5 days). Nanofibers without growth factor or electrical stimulation were used as control.

Under the unstimulated condition, most PC12 cells remained undifferentiated on the PS-PANi-1 meshes (Fig. 7A). However, there were neurites formed on the sample of NGF-loaded PS-PANi-1 meshes (Fig. 7B); these results suggested that NGF release could stimulate PC12 cell differentiation. Compared with the unstimulated condition, PC12 cells also showed neurite outgrowth on the PS-PANi-1 meshes, which meant that electrical stimulation might also stimulate PC12 cell differentiation (Fig. 7C). While the mechanism of electrical stimulation promoting neurite formation was not fully understood, our result may provide insight for further study. PC12 cells exhibited more and longer neurite outgrowth, which demonstrated that NGF and electrical stimulation could have a significant effect on PC12 cell differentiation (Fig. 7D). In addition, neurite outgrowth also occurred along the major axis direction of the conductive nanofibers, which suggested that the aligned structure, electrical

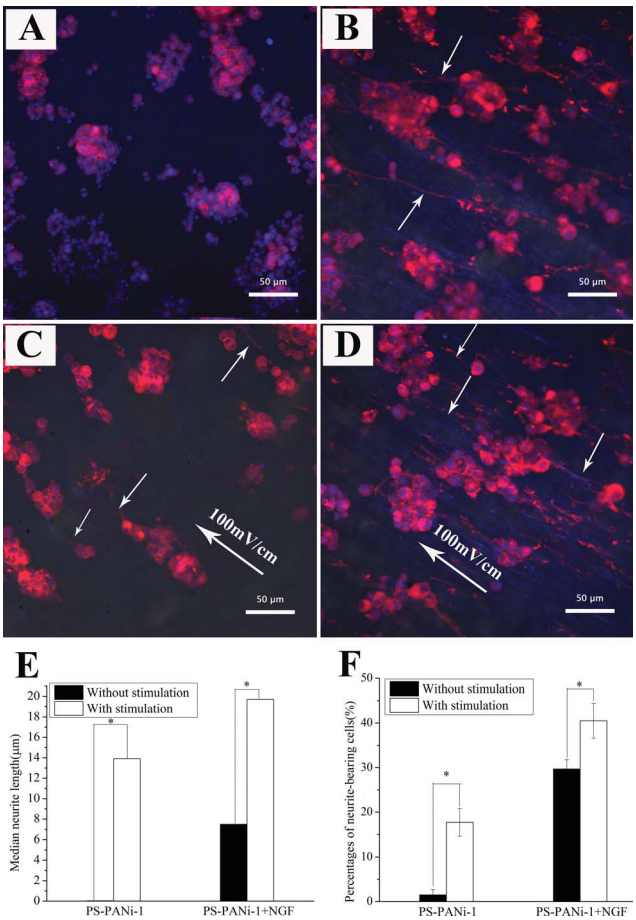

Fig. 7 Fluorescent images of PC12 cells cultured on the surface of aligned nanofibers with labeling of cytoplasm (red) and nuclei (blue). (A) & (C) PS-PANi-1; (B) & (D) NGF-loaded PS-PANi-1; (C) & (D) cells stimulated with 100 mV cm^{-1} for 5 days (1 h each day), scale bar = 50 μm. (E) Median neurite length and (F) percentage of neurite-bearing PC12 cells on the PS-PANi-1 nanofibers (* = significantly different in comparison with no stimulation, $p < 0.05$, $n = 4$).

stimulation and NGF could have a dramatic effect in enhancing neurite outgrowth of PC12 cells. Lee *et al.* and Xia *et al.* also found a similar trend with PC12 and dorsal root ganglia (DRG) cells. In their studies, the random and aligned fibers did not have a significant effect on the numbers of neurites.[9,41]

To quantify the differentiation of the neurites, the neurite length and percentage of neurite-bearing PC12 cells were calculated. Neurite length was measured by a linear distance between the tip of the neurite and the cell junction. Because the neurite lengths were not normally distributed, the median neurite length was used as a measure of neurite outgrowth. Under the unstimulated condition, the median neurite length increased from 0.04 to 13.9 μm and the percentage of neurite-bearing cells increased from 1.5 ± 1.2% to 29.7 ± 2.1% for cells cultured on PS-PANi-1 and NGF-loaded PS-PANi-1 meshes, respectively. Whereas, under the electrically stimulated condition, the median neurite length increased from 7.5 to 19.7 μm and the percentage of neurite-bearing cells increased from 17.7 ± 3.1% (PS-PANi-1) to 40.5 ± 3.9% (NGF-loaded PS-PANi-1), respectively. There was a significant increase in both median neurite length and percentage of neurite-bearing cells with electrical stimulation in comparison to that without electrical stimulation as shown in Fig. 7E and F. These results confirmed that NGF and electrical stimulation both play a significant role in the differentiation of neurites. In addition, a combination of NGF and electrical stimulation was more effective in promoting PC12 differentiation, which suggested the potential use of well-aligned conductive core–shell structure nanofibrous scaffolds in neural tissue engineering.

3.4 NGF release from PS/PANi composites

The cumulative NGF release was observed for 5 days with and without electrical stimulation as shown in Fig. 8A. According to the figure, NGF release showed similar patterns regardless of electrical stimulation, but the released NGF amount increased significantly with electrical stimulation. Although the exact effects of electrical stimulation on NGF release from core–shell nanofibers have not been fully understood, similar trends have been demonstrated by Im *et al.*, Thompson *et al.* and Cho *et al.* and they reported that the released drug amount increased effectively at higher applied electric voltages.[8,28,43] Therefore, we speculated that electrical stimulation might also increase the conductive core–shell structure nanofiber release behavior.

The bioactivity of the NGF release from electrospun NGF-loaded PS/PANi fibers was analyzed by observing the differentiation of PC12 cells into neurites. The PC12 cells were cultured in 5 days sustained-release medium for 3 days and the cells cultured in RPMI 1640 medium were used as the negative

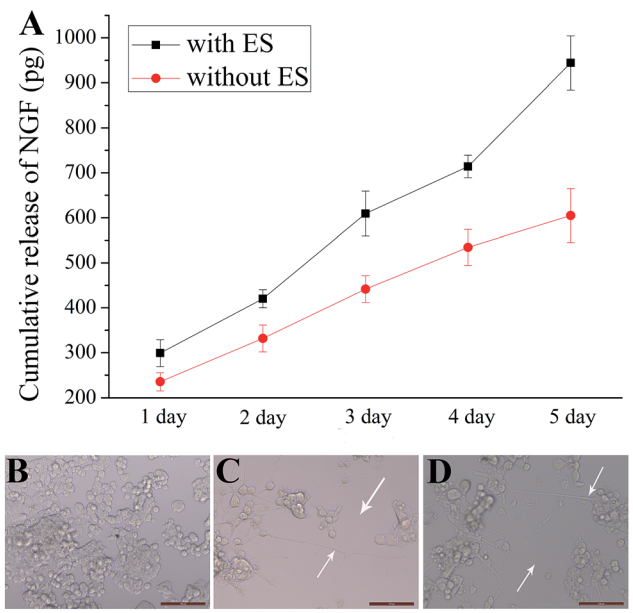

Fig. 8 (A) Cumulative release of NGF from the PS-PANi-1 + NGF nanofibers with and without electrical stimulation. PC-12 differentiation in different culture media for 3 days: (B) RPMI 1640 medium; (C) RPMI 1640 medium containing NGF sustained-release medium (5 days) without electrical stimulation; (D) RPMI 1640 medium containing NGF sustained-release medium (5 days) with electrical stimulation at a constant voltage of 100 mV cm^{-1} (5 days, 1 h per day), scale bar = 100 μm, $n = 6$.

control. Most cells retained a typical circular morphology in the negative control (Fig. 8B). However, neuronal differentiation was observed in the cells cultured in 5 days sustained-release medium with or without electrical stimulation (Fig. 8C and D). The results demonstrated that the released NGF from the PS-PANi-1 nanofibers retains its bioactivity with or without electrical stimulation. Therefore, a constant voltage of 100 mV cm^{-1} would not affect the bioactivity of the released NGF.

4 Conclusion

Conductive polymers have great potential for fabricating stimulus-responsive scaffolds. In this study, we prepared highly aligned conductive PS/PANi nanofibers and NGF-loaded PS/PANi nanofibers by a coaxial electrospinning technique, and investigated their effects on the proliferation of Schwann cells and differentiation of PC12 cells. The topographical cue of fiber alignment had a direct effect on cellular morphologies. Schwann cells had the highest proliferation speed on NGF-loaded PS-PANi-1 nanofibers. In addition, a high content of PANi induced toxicity to Schwann cells while the incorporation of NGF in PS/PANi could decrease the toxic effect of PANi on Schwann cells. The PC12 cells were used to assess the neurite outgrowth and axon elongation on NGF-loaded PS-PANi-1 nanofibrous scaffolds under unstimulated and stimulated conditions. PC12 cells exhibited more and longer neurites under the stimulated condition. NGF release and electrical stimulation could exert a synergistic effect on PC12 cell differentiation. To the best of our knowledge, our study suggests that electrical stimulation could increase NGF release from conductive core–shell nanofibers, and this release model might also be applied for a drug delivery system which could be used in an electrically controlled manner. Therefore, our results provide a new way to create functional scaffolds for nerve tissue regeneration.

Acknowledgements

This work was supported by the National Natural Science Foundation of China (Grant no. 31271035 and 31470941), the Science and Technology Commission of Shanghai Municipality Program (Grant no. 11nm0506200) and Ph.D. Programs Foundation of Ministry of Education of China (20130075110005), and the independent Design Project of Key Scientific and Technological Innovation Team of Zhejiang Province (no. 2010R50012-19). The authors would like to extend their sincere appreciation to the Deanship of Scientific Research at King Saud University for its funding of this research through the research group project no. RGP-201.

Notes and references

1 Y. Gu, J. Zhu, C. Xue, Z. Li, F. Ding, Y. Yang and X. Gu, *Biomaterials*, 2014, **35**, 2253–2263.
2 M. Z. Entong Wang, J. V. Forrester and C. D. McCaig, *Exp. Eye Res.*, 2003, **76**, 29–37.
3 C. Schmidt, V. Shastri, J. Vacanti and R. Langer, *Proc. Natl. Acad. Sci. U. S. A.*, 1997, **94**, 8948–8953.
4 E. Mooney, J. Mackle, D. Blond, E. O'Cearbhaill, G. Shaw, W. Blau, F. Barry, V. Barron and J. Murphy, *Biomaterials*, 2012, **33**, 6132–6139.
5 R. Balint, N. J. Cassidy and S. H. Cartmell, *Acta Biomater.*, 2014, **10**, 2341–2353.
6 H. Xu, J. M. Holzwarth, Y. Yan, P. Xu, H. Zheng, Y. Yin, S. Li and P. X. Ma, *Biomaterials*, 2014, **35**, 225–235.
7 M. D. M. Brett Runge, *Biomacromolecules*, 2010, **11**, 2845–2853.
8 Y. Cho and R. Ben Borgens, *J. Mater. Chem. B*, 2013, **1**, 4166.
9 J. Y. Lee, C. A. Bashur, A. S. Goldstein and C. E. Schmidt, *Biomaterials*, 2009, **30**, 4325–4335.
10 S. Shao, S. Zhou, L. Li, J. Li, C. Luo, J. Wang, X. Li and J. Weng, *Biomaterials*, 2011, **32**, 2821–2833.
11 M. Sebaa, T. Y. Nguyen, S. Dhillon, S. Garcia and H. Liu, *J. Biomed. Mater. Res., Part A*, 2014, DOI: 10.1002/jbm.a.35142.
12 Y. Su, Q. Su, W. Liu, M. Lim, J. R. Venugopal, X. Mo, S. Ramakrishna, S. S. Al-Deyab and M. El-Newehy, *Acta Biomater.*, 2012, **8**, 763–771.
13 C.-Y. Wang, J.-J. Liu, C.-Y. Fan, X.-M. Mo, H.-J. Ruan and F.-F. Li, *J. Biomater. Sci., Polym. Ed.*, 2012, **23**, 167–184.
14 S. Y. Chew, R. Mi, A. Hoke and K. W. Leong, *Biomaterials*, 2008, **29**, 653–661.
15 Z. Yin, X. Chen, J. L. Chen, W. L. Shen, T. M. Hieu Nguyen, L. Gao and H. W. Ouyang, *Biomaterials*, 2010, **31**, 2163–2175.
16 B. Wang, Q. Cai, S. Zhang, X. Yang and X. Deng, *J. Mech. Behav. Biomed. Mater.*, 2011, **4**, 600–609.
17 T. Schneider, B. Kohl, T. Sauter, K. Kratz, A. Lendlein, W. Ertel and G. Schulze-Tanzil, *Clin. Hemorheol. Microcirc.*, 2012, **52**, 325–336.
18 M. Li, Y. Guo, Y. Wei, A. MacDiarmid and P. Lelkes, *Biomaterials*, 2006, **27**, 2705–2715.
19 S. I. Jeong, I. D. Jun, M. J. Choi, Y. C. Nho, Y. M. Lee and H. Shin, *Macromol. Biosci.*, 2008, **8**, 627–637.
20 S. H. Bhang, S. I. Jeong, T. J. Lee, I. Jun, Y. B. Lee, B. S. Kim and H. Shin, *Macromol. Biosci.*, 2012, **12**, 402–411.
21 C. W. Hsiao, M. Y. Bai, Y. Chang, M. F. Chung, T. Y. Lee, C. T. Wu, B. Maiti, Z. X. Liao, R. K. Li and H. W. Sung, *Biomaterials*, 2013, **34**, 1063–1072.
22 M. C. Chen, Y. C. Sun and Y. H. Chen, *Acta Biomater.*, 2013, **9**, 5562–5572.
23 J.-G. Zhang and X.-M. Mo, *Front. Mater. Sci.*, 2013, **7**, 129–142.
24 C. Y. Wang, K. H. Zhang, C. Y. Fan, X. M. Mo, H. J. Ruan and F. F. Li, *Acta Biomater.*, 2011, **7**, 634–643.
25 K. Zhang, H. Wang, C. Huang, Y. Su, X. Mo and Y. Ikada, *J. Biomed. Mater. Res., Part A*, 2010, **93**, 984–993.
26 J. W. Sing Yian Chew, E. K. F. Yim and K. W. Leong, *Biomacromolecules*, 2005, **6**, 2017–2024.
27 W. Sun, C. Sun, H. Lin, H. Zhao, J. Wang, H. Ma, B. Chen, Z. Xiao and J. Dai, *Biomaterials*, 2009, **30**, 4649–4656.
28 B. C. Thompson, R. T. Richardson, S. E. Moulton, A. J. Evans, S. O'Leary, G. M. Clark and G. G. Wallace, *J. Controlled Release*, 2010, **141**, 161–167.
29 C. Correia, S. Bhumiratana, L. P. Yan, A. L. Oliveira, J. M. Gimble, D. Rockwood, D. L. Kaplan, R. A. Sousa, R. L. Reis and G. Vunjak-Novakovic, *Acta Biomater.*, 2012, **8**, 2483–2492.

30 L. Ghasemi-Mobarakeh, M. Prabhakaran, M. Morshed, M. Nasr-Esfahani and S. Ramakrishna, *Tissue Eng., Part A*, 2009, **15**, 3605–3619.
31 I. Jun, S. Jeong and H. Shin, *Biomaterials*, 2009, **30**, 2038–2047.
32 M. S. Laleh Ghasemi-Mobarakeh, M. P. Prabhakaran, M. Morshed, P. D. Mohammad Hossein Nasr-Esfahani and S. Ramakrishna, *Tissue Eng., Part A*, 2009, **15**, 3605–3619.
33 J. B. Leach, X. Q. Brown, J. G. Jacot, P. A. Dimilla and J. Y. Wong, *J. Neural Eng.*, 2007, **4**, 26–34.
34 Y. Zhu, J. Zhang, Y. Zheng, Z. Huang, L. Feng and L. Jiang, *Adv. Funct. Mater.*, 2006, **16**, 568–574.
35 D. Kai, M. P. Prabhakaran, G. Jin and S. Ramakrishna, *J. Mater. Chem. B*, 2013, **1**, 2305–2314.
36 R. R. Vankayala, W.-J. P. Lai, K.-C. Cheng and K. C. Hwang, *Polymer*, 2011, **52**, 3337–3343.
37 Z. Ping, *J. Chem. Soc., Faraday Trans.*, 1996, **92**, 3063–3067.
38 M. Farokhi, F. Mottaghitalab, M. A. Shokrgozar, J. Ai, J. Hadjati and M. Azami, *Mater. Sci. Eng., C*, 2014, **35**, 401–410.
39 F. Cilurzo, C. G. Gennari, F. Selmin, L. A. Marotta, P. Minghetti and L. Montanari, *Int. J. Pharm.*, 2011, **414**, 218–224.
40 N. K. Guimard, N. Gomez and C. E. Schmidt, *Prog. Polym. Sci.*, 2007, **32**, 876–921.
41 J. Xie, M. R. Macewan, S. M. Willerth, X. Li, D. W. Moran, S. E. Sakiyama-Elbert and Y. Xia, *Adv. Funct. Mater.*, 2009, **19**, 2312–2318.
42 J. Zeng, Z. Huang, G. Yin, J. Qin, X. Chen and J. Gu, *Colloids Surf., B*, 2013, **110**, 450–457.
43 J. S. Im, B. Bai and Y. S. Lee, *Biomaterials*, 2010, **31**, 1414–1419.